Available online at www.sciencedirect.com
SCIENCE DIRECT®
Thermochimica Acta 424 (2004) 15–23
thermochimica acta
www.elsevier.com/locate/tca

Structure and thermal evolution of Mg–Al layered double hydroxide containing interlayer organic glyphosate anions

Feng Li [a,1], Lihong Zhang [a], David G. Evans [a], Claude Forano [b], Xue Duan [a,*]

[a] *The Key Laboratory of Science and Technology of Controllable Chemical Reactions, Ministry of Education, Beijing University of Chemical Technology, Beijing 100029, PR China*
[b] *Laboratoire des Matériaux Inorganiques, UPRES-A 6002, Université Blaise Pascal, 63177 Aubière Cedex, France*

Received 8 March 2004; received in revised form 11 May 2004; accepted 11 May 2004
Available online 24 June 2004

Abstract

Layered double hydroxide (LDH) with the Mg^{2+}/Al^{3+} molar ratio of 2.0 containing interlayer organic pesticide glyphosate anions (MgAl–Gly–LDH) has been synthesized by the use of anion exchange and coprecipitation routes. Intercalation experiments with glyphosate (Gly) reveal a correlation between the temperatures for thermal treatments and the types of reaction it undergoes with Gly. The grafting of the Gly anion onto hydroxylated sheets of LDH by moderate thermal treatments (hydrothermal treatments and calcinations) was confirmed by a combination of several techniques, including powder X-ray diffraction (XRD), Fourier transform infrared spectroscopy (FT-IR), thermogravimetry analysis (TGA–DTG), and ^{31}P nuclear magnetic resonance (NMR). The thermal decomposition of MgAl–Gly–LDH results in the removal of loosely held interlayer water, grafting reaction between the interlayer anions and hydroxyl groups on the lattice of LDH, dehydroxylation of the lattice and decomposition of the interlayer species in succession, thus leading to a variety of crystallographic transitions.

Keywords: Layered double hydroxide; Glyphosate; Intercalation; Grafting; Thermal decomposition

1. Introduction

Widespread use of pesticides in modern agriculture is of serious environmental concern because of their toxicity. To ensure adequate pest control for a sufficient period, pesticides are applied in greatly exceeding amount, but much of the amount of pesticide is wasted due to losses resulting from physical, chemical, and biological processes [1]. The excessive quantities added increase the likelihood of runoff or leaching and thus lead to the pollution of surface or subsurface water [2]. For example, the pesticide, *N*-(phosphonomethyl)glycine (glyphosate), is widely used in agriculture and has been detected in surface and subsurface water [3]. However, the danger can be reduced by improved pest control practices including reduction in the amount of active ingredient. In many cases, the use of controlled-release pesticide formulations can supply active ingredient at the required rate, thus reducing the amount of chemical needed for pest control, and decreasing the risk to the environment. In general, controlled release of pesticides can permit safer, more efficient, and more economical crop protection [4].

Layered double hydroxides (LDHs), also known as hydrotalcite-like materials, are a class of synthetic two-dimensional nanostructured anionic clays whose structure can be described as containing brucite-like layers, where a fraction of the divalent cations coordinated octahedrally by hydroxyl groups have been replaced isomorphously by trivalent cations giving positively-charged lattice with charge-balancing anions between the layers, and some hydrogen bonded water molecules may occupy the other remaining free space of the interlayer region [5–7]. LDHs may be represented by the general formula $[M^{2+}_{1-x}\,M^{3+}_{x}(OH)_2]^{x+}(A^{n-})_{x/n}\cdot mH_2O$, where M^{2+} (Mg, Fe, Co, Cu,

* Corresponding author. Tel.: +86 10 64412109; fax: +86 10 64425385.
E-mail addresses: lifeng_70@163.com, duanx@mail.buct.edu.cn (X. Duan).
[1] Co-corresponding author.

0040-6031/$ – see front matter © 2004 Elsevier B.V. All rights reserved.
doi:10.1016/j.tca.2004.05.007

Ni, or Zn) and M^{3+} (Al, Cr, Ga, Mn or Fe) are di- and tri-valent cations, respectively; *x* is equal to the molar ratio of $M^{2+}/(M^{2+} + M^{3+})$ in the range of 0.2–0.33; and A^{n-} is an anion. Various anionic species have been intercalated into the gallery region of LDHs mainly by coprecipitation or ion exchange, e.g. inorganic acids [8,9], organic acids [10,11], anionic polymers [12], cyclodextrin [13], and reduced C_{60} [14]. These layered LDH solids based upon the alternation of inorganic and organic interlayer species have received considerable attention, because of their many practical applications, including as catalysts [15], functional materials [16], and nanocomposite materials [17]. The attractive feature of such materials is that the host layers can impose restricted geometry on the interlayer guests leading to enhance control of stereochemistry, rates of reaction, and product distributions. Many species can be assembled by reaction of guest species in the LDH matrixes [16]. Therefore the study of advanced materials based on LDHs is a rapidly growing field, and has application in areas such as separation science [18,19], in situ polymerization [12,20], and photochemistry [21].

Organic intercalates in inorganic host structures of LDHs are considered as one class of hybrid compounds. Under topotactic ion substitution, the organic partner is introduced in the inorganic matrix, with the retention of the overall structure. From a structural point of view, layered hybrid materials combine all the benefits of both the layered host with its expansion and surface properties and interstratified 2D organic domain with its ability to adsorb organic materials. As much as LDHs play an important role in ion exchange and adsorption of organic molecules, it is rather possible that LDH materials can be used as potential matrixes in modeling controlled-release pesticide formulations through the intercalation of pesticide molecules. Although controlled-release pesticide formulations are usually used at room temperature, anionic functions (phosphonate and carboxylate) of glyphosate (Gly) molecule are well known to be sensitive to temperatures. As a result, the structure and property of as-produced pesticide formulations depend to a large extent on the thermal treatments. Therefore, insight into the chemical stability of these hybrid intercalates is vital, and the knowledge of the reactivity with regard to the organic functional groups of pesticides must be envisaged. In the present work, the intercalation characteristics of organic Gly anion into Mg–Al layered double hydroxide were evaluated under different conditions for thermal treatments with particular attention to the arrangement of the charge-balancing anions, and the thermal evolution of intercalate structure was also studied.

2. Experimental

2.1. Preparation of samples

Mg–Al layered double hydroxide nitrate (MgAl–NO_3–LDH) was prepared by the coprecipitation method under nitrogen atmosphere (in order to minimize the contamination with atmospheric CO_2). Fifty milliliters of aqueous Mg and Al nitrate solution with the experimental Mg^{2+}/Al^{3+} molar ratio of 2.0 was added dropwise to a flask containing 200 mL of deionized water, then a base solution of sodium hydroxide (1 M) was simultaneously added to fix the pH of coprecipitation at 10.0 ± 0.1. The addition of the metallic salt solution was completed in 4 h. The resulting precipitate obtained was aged for 24 h at room temperature, and then recovered by four dispersion and centrifugation cycles in deionized water, and finally the obtained gelatinous precipitate was air-dried.

Mg–Al layered double hydroxide intercalated with organic Gly ions (MgAl–Gly–LDH) was prepared by coprecipitation method under nitrogen atmosphere and vigorous magnetic stirring. Fifty milliliters of aqueous Mg and Al nitrate solution with the experimental Mg/Al molar ratio of 2.0 was added dropwise to 200 mL of deionized water, where an excess of 2.5 times equivalence of Gly over Al^{3+} content was used. The pH of mixture was held constant at 10.0 ± 0.1 by simultaneous addition of a base solution of sodium hydroxide (1 M). The resulting precipitate obtained was aged for 24 h at room temperature, recovered by four dispersion and centrifugation cycles in deionized water. Finally, the obtained gelatinous precipitate was air-dried.

MgAl–Gly–LDH was also prepared through an anion exchange route. Under nitrogen atmosphere and vigorous magnetic stirring, an aqueous solution of Gly with an excess of 2.5 times equivalence of Gly anions over Al^{3+} content in MgAl–NO_3–LDH was added dropwise into 200 mL of deionized water where LDH-nitrate precursor has been dispersed. The pH of mixture was held constant at 10.0 ± 0.1 by simultaneous addition of 1 M sodium hydroxide solution. The exchange process was kept at room temperature for 24 h. The precipitate was recovered by four dispersion and centrifugation cycles in deionized water, and finally was air-dried or calcined at 120, 350, 500 and 700 °C for 12 h in air, respectively. In addition, after ion exchange the precipitate was also treated hydrothermally at 60, 120 and 150 °C for 24 h, respectively. Finally, the precipitate was recovered by four dispersion and centrifugation cycles in deionized water, and finally was air-dried.

Mg–Al layered double hydroxide carbonate (MgAl–CO_3–LDH) was prepared by coprecipitation method. Fifty milliliters of aqueous Mg and Al nitrate solution with the experimental Mg^{2+}/Al^{3+} molar ratio of 2.0 was added dropwise to 200 mL of 0.4 M sodium carbonate solution. The pH of mixture was held constant at 10.0 ± 0.1 by simultaneous addition of 1 M sodium hydroxide solution. The addition of the metallic salt solution was completed in 4 h. The resulting precipitate obtained was aged for 24 h at room temperature, and then recovered by four dispersion and centrifugation cycles in deionized water, and finally the obtained gelatinous precipitate was air-dried.

2.2. Characterization

Powder X-ray diffraction (XRD) patterns for the samples were recorded using a Rigaku XRD-6000 diffractometer under the following conditions: 40 kV, 30 mA, Cu Kα radiation ($\lambda = 0.15418$ nm). The samples were step-scanned in steps of 0.04° (2θ) using a count time of 10 s/step. The observed interplanar spacings were corrected using elemental Si as an internal standard [$d(1\,1\,1) = 0.31355$ nm; JCPDS file no. 27-1402]. In situ high temperature powder X-ray diffraction (HT-XRD) experiment was carried out on a Rigaku D/MAX2500VB2 + /PC diffractometer in the temperature range of 25–1200 °C under vacuum (10^{-2} Torr) at a rate of 0.5 °C/s. The sample was equilibrated at any given temperature for 30 min.

Elemental analysis for metal ions and P in LDHs was performed using a Shimadzu ICPS-75000 inductively coupled plasma emission spectrometer (ICP-ES). The N-content in LDHs was determined by Elementar Vario EL analyzer under the following conditions: carrier gas current 20 mL/min, oxygen current 20 mL/min, combustion temperature 950 °C and reduction temperature 550 °C.

Fourier transform infrared (FT-IR) spectra were recorded in the range 4000–400 cm^{-1} with 2 cm^{-1} resolution on a Bruker Vector-22 Fourier transform spectrometer using the KBr pellet technique (1 mg of sample in 100 mg of KBr).

Thermogravimetry analysis (TGA–DTG) was carried out in air on a PCT-1A thermal analysis system produced locally. Samples of 9.0–10.0 mg were heated at a rate 5 °C/min up to 800 °C.

The ^{31}P nuclear magnetic resonance (NMR) spectra were recorded with a Varian Unity Inova 300 spectrometer operating at 121.4 MHz under CP MAS conditions. The chemical shifts were referenced to an external H_3PO_4 solution (85%) at 0.0 ppm.

3. Results and discussion

3.1. Intercalation

The powder XRD patterns for MgAl–NO_3–LDH and intercalated MgAl–Gly–LDH samples are shown in Fig. 1, whilst Table 1 summarizes the structural and analytical data of LDHs. Obviously, in three cases the XRD patterns are typical of hydrotalcite-like layered double hydroxide (JCPDF file no. 38-0487) materials [22], exhibit the sharp characteristic diffraction lines appearing as symmetric lines at low 2θ angle, which are ascribed to diffractions by planes (0 0 3), (0 0 6) and/or (0 0 9), corresponding to the basal spacing and its higher order diffractions. All of the main characteristic diffractions of the intercalated sample prepared by ion exchange are similar with those of the intercalated one by coprecipitation. Compared to the XRD patterns for MgAl–NO_3–LDH, those for the intercalated samples show out a smaller degree displacement of (0 0 3) diffraction line denoting an increase in the basal spacing (d_{003}) from 0.89 to 1.22 nm, which is due to the intercalation of Gly anion, and hence an expanded intercalate is formed. However, the crystallinity of the organic intercalate is lowered, as attested by the widening of the remaining XRD lines. In addition, it can be also noted that two tiny bulgy peaks at 2θ angles of 9.87 and 19.78° for the intercalated sample

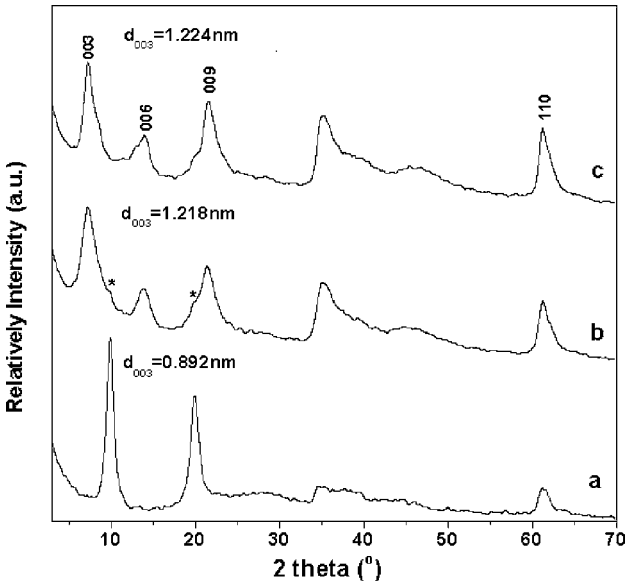

Fig. 1. XRD patterns for: (a) MgAl–NO_3–LDH, MgAl–Gly–LDH by anion exchange ((b) (*) MgAl–NO_3–LDH impurity), and (c) MgAl–Gly–LDH by coprecipitation.

Table 1
Analytical and structural data for the synthesized LDHs

Samples	d_{003} (nm)	Final Mg/Al /P/N molar ratio[c]	Theoretical Al/P molar ratio[d]	Theoretical Al/P molar ratio[e]
MgAl–NO_3–LDH	0.892	1.94:1:0:1	–	–
MgAl–Gly–LDH[a]	1.224	2:1:0.4:0.4	1:0.5	1:0.33
MgAl–Gly–LDH[b]	1.218	1.93:1:0.39:0.39	1:0.5	1:0.33

[a] Coprecipitation.
[b] Ion exchange.
[c] Determined by elemental analysis.
[d] Calculated when interlayer anion is divalent Gly anion according to charge balance in an LDH.
[e] Calculated when interlayer anion is trivalent Gly anion.

prepared by ion exchange, which are ascribed to the (0 0 3) and (0 0 6) diffraction lines for MgAl–NO_3–LDH, represent a very small amount of unreacted LDH-nitrate impurity.

Elemental analysis (see Table 1) shows that the final Al/P molar ratios in the intercalated products are between two theoretical values calculated according to charge balance in an LDH when interlayer anion is trivalent Gly anion and divalent Gly anion, individually, considering that the amount of LDH-nitrate impurity could be ignored due to the fact that the final P/N molar ratio of 1.0 in the intercalated sample is determined to the same value as that in Gly molecule itself. It suggests that trivalent and divalent Gly anions coexist in the intercalated samples. As a result, both forms of Gly anions with the $(O_2CCH_2NHCH_2PO_3)^{3-}/(O_2CCH_2NH_2CH_2PO_3)^{2-}$ molar ratios of 1.0 for the coprecipitated sample and 1.3 for the exchanged one may be intercalated into the interlayer domain of the LDHs. This is expected on the basis of the fact that Gly molecule is amphoteric, ranging from univalent positive charge to trivalent negative charge, and exhibits the following aqueous dissociation constants: $pK_1 < 2$, $pK_2 = 2.6$, $pK_3 = 5.6$ and $pK_4 = 10.6$ [3]. Therefore, under synthesis conditions (pH = 10.0) the species exist predominantly as $(O_2CCH_2NHCH_2PO_3)^{3-}$ anion and/or $(O_2CCH_2NH_2CH_2PO_3)^{2-}$ anion, considering that the real pH within the layers is higher than that measured with a pH meter outside them.

The interlayer distance is mainly determined by the orientation of the anions in the interlayer domain, which can be simulated from comparison of the gallery height of the remaining interlayer occupied by the intercalated anions and the size of intercalated anion. The value of the gallery height can be obtained from the difference between the basal spacing and thickness of layers. Assuming the thickness of the brucite-like layer is approximately 0.48 nm [23], this suggests that the gallery height is close to 0.74 nm including the hydrogen domains on both sides of the layers. Given that the most stable conformers of Gly molecule show pinched conformations on the basis of an ab initio MO study [24], the length of representative conformer of Gly anion calculated (see Fig. 2a) is approximately 0.45 nm near to the value of 0.43 nm reported by Martín et al. [3], such a value may be associated with the formation of vertical intertwined single layers of Gly anions in the interlayer domain, with anionic functions (phosphonate and carboxylate) of Gly anions attached to the hydroxylated lattice through strong hydrogen bonding and electrostatic attraction between interlayer anions and positively-changed lattice of LDH. Gly anion with a rigid molecular structure has been used in order to facilitate the description of structure, and thus Fig. 2a presents schematic diagram of arrangement of interlayer Gly anions.

This intercalation reaction is also supported by the FT-IR results. The FT-IR spectra of MgAl–Gly–LDH, MgAl–NO_3–LDH and Gly molecule in the region between 400 and 4000 cm^{-1} are illustrated in Fig. 3. In general the strong and broad band observed around 3600–3200 cm^{-1} centered at 3460 cm^{-1} corresponds to the O–H stretching vibration of surface and interlayer water molecules [6], which are found at lower frequency in LDHs compared with the O–H stretching vibration in free water at 3600 cm^{-1} [25]. This is related to the formation of hydrogen bonding of interlayer water with the guest anions as well as with hydroxide groups of layers [26]. Moreover, the absorption is appreciably broadened by the presence of the interlayer Gly anion, due to the interaction of the multifunctional groups of Gly anion with water molecules as well as the interlayer matter disorder [27,28], resulting in several kinds of hydroxyl-stretching vibrations with a broad distribution of absorption frequency. The absorption at 1630 cm^{-1} is assigned to the bending vibration of water. The bands observed in the low-frequency region of the spectrum are interpreted as the lattice vibration modes and can be attributed to M–O from 850 to 600 cm^{-1} and O–M–O near 440 cm^{-1} vibrations [29]. The proof for the presence of phosphonate groups

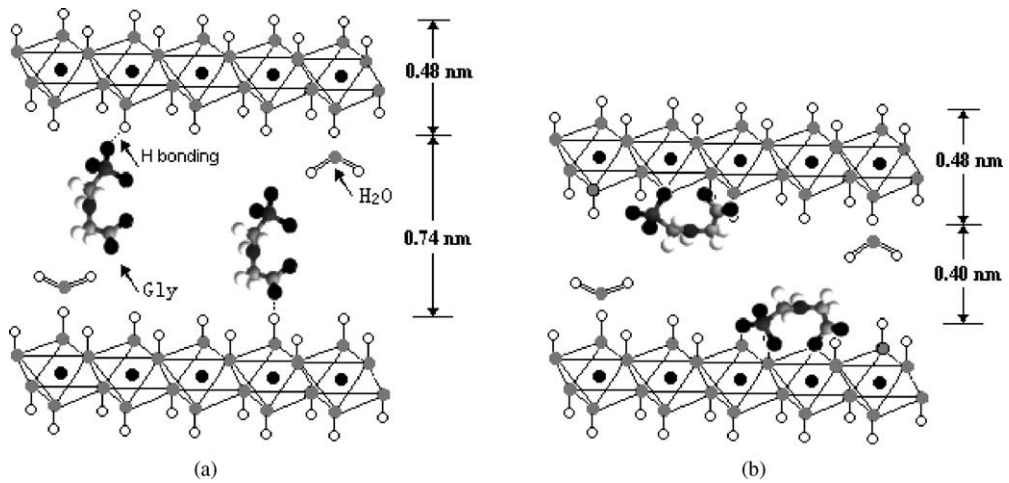

Fig. 2. Schematic diagrams of interlayer arrangement of: (a) MgAl with Gly anions; and (b) grafted Gly anions.

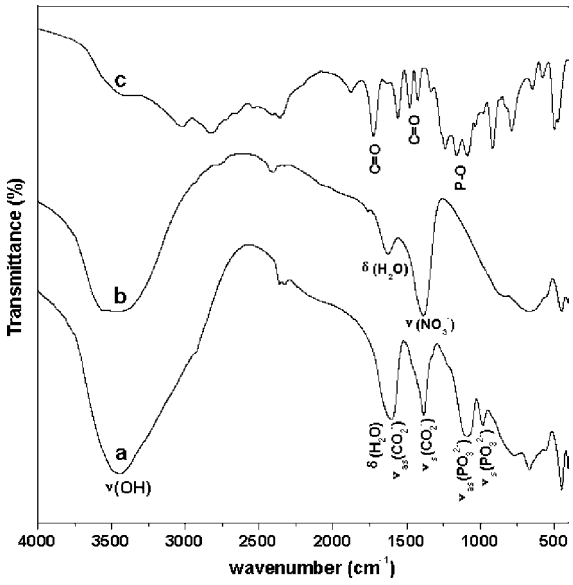

Fig. 3. FT-IR spectra of: (a) MgAl–Gly–LDH, (b) MgAl–NO_3–LDH and (c) Gly molecule.

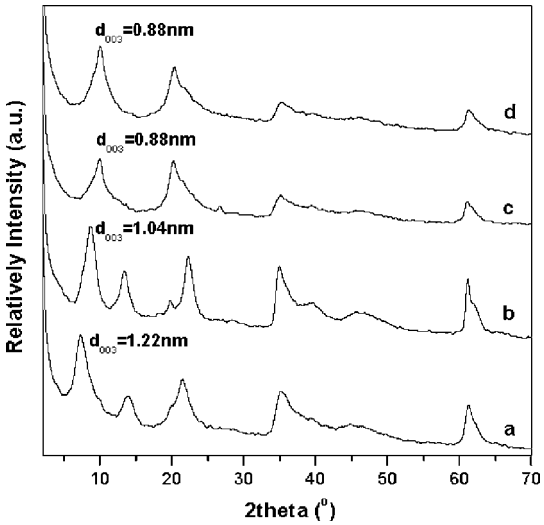

Fig. 4. XRD patterns for the MgAl–Gly–LDHs at different hydrothermal temperature: (a) room temperature, (b) 60 °C, (c) 120 °C and (d) 150 °C.

results from their characteristic vibrations: ν_s (PO_3^{2-}) at 984 cm^{-1} and ν_{as} (PO_3^{2-}) at 1087 cm^{-1}. Compared with the symmetric and anti-symmetric vibrations of –PO_3^{2-} of Gly molecule, those of the intercalated sample displays broadened bands, which can possibly be attributed to stronger hydrogen bonding with interlayer water molecules. Meanwhile, there is an absorption at 1383 cm^{-1}, which is associated with the symmetric vibration of the anionic carboxylate functions (–CO_2^-) of interlayer Gly anions. In addition, the broad and strong absorption band around 1640–1580 cm^{-1} centered at 1600 cm^{-1} should actually be associated with a superposition of water deformation, δ (H_2O), and anti-symmetric vibration of the anionic carboxylate functions (–CO_2^-) [30].

3.2. Thermal treatments

Fig. 4 shows the XRD patterns for the intercalated samples treated hydrothermally at 60, 120 and 150 °C, respectively. Note that after the hydrothermal treatment of 60 °C the exchanged compound shows an interlayer distance of 1.04 nm. However, two intense diffractions at 13.3 and 22.3° do not belong to (0 0 6) and (0 0 9) higher order diffractions of the (0 0 3) diffraction at 8.7° according to the relation among diffraction lines ($d_{003} = 2d_{006} = 3d_{009}$). The result suggests that multiple crystalline phases in the treated sample coexist. When the sample is treated at 120 °C or above, the XRD patterns exhibit the sharp characteristic (0 0 3) diffraction line with its corresponding (0 0 6) higher order diffraction, and the value of d_{003} decreases to 0.88 nm. As it is rather difficult for Gly anion to fit in such shorter gallery height (0.40 nm) with the hydrogen bonding domains on both sides of the layers, obviously, reaction between host and guest partners should have occurred. Considering that a developed layered structure along the *c*-axis has been concluded in the intercalated sample because of many 0 0 *l*-type lines, the extent of the stacking layer in the hydrothermally-treated sample is relatively small. The above results imply that the hydrothermal treatment leads to a sandwich structure where alternate mineral and organic domains are stacked. The interlayer contraction can be explained by the grafting of interlayer organic anions onto the hydroxylated layers through the substitution of OH groups on the layers.

On the FT-IR spectra for the samples (see Fig. 5), the intensities of the interlayer water bands at 3460 and 1630 cm^{-1} do not change with temperature for hydrothermal treatment above 60 °C. This means that the amount of interlayer water in the intercalated sample is always constant. Meanwhile, the

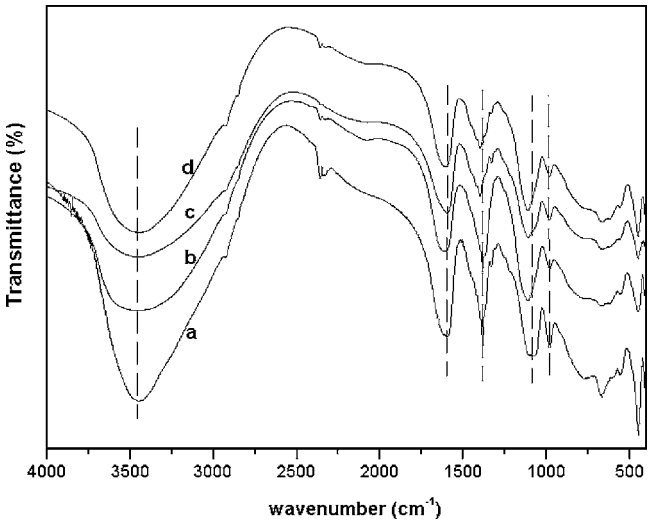

Fig. 5. FT-IR spectra for MgAl–Gly–LDHs at different hydrothermal temperature: (a) room temperature, (b) 60 °C, (c) 120 °C and (d) 150 °C.

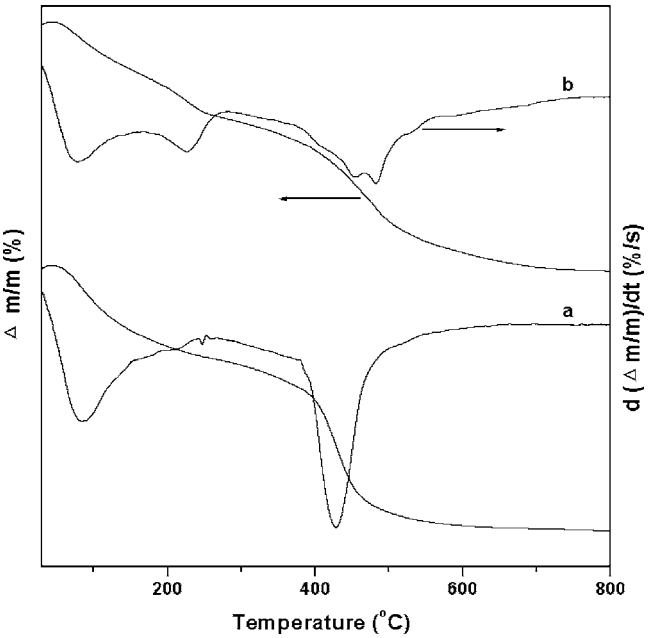

Fig. 6. TGA–DTG curves for: (a) MgAl–Gly–LDH and (b) MgAl–Gly–LDH treated hydrothermally at 120 °C.

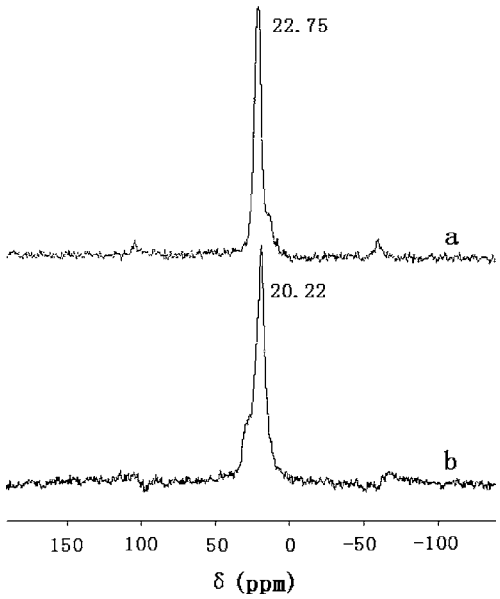

Fig. 7. ^{31}P NMR spectra for: (a) MgAl–Gly–LDH and (b) MgAl–Gly–LDH treated hydrothermally at 120 °C.

characteristic stretching vibration of the $-CO_2^-$ functions of Gly anions at 1383 cm^{-1} begins to shift to 1401 cm^{-1} with temperature for hydrothermal treatment above 120 °C, and the characteristic vibration of the anionic $-PO_3^{2-}$ functions at 1087 cm^{-1} also shift to 1099 cm^{-1}. It indicates that with temperature the anionic $-CO_2^-$ and $-PO_3^{2-}$ functions of interlayer Gly anions begin to interact more strongly with the backbone of LDH itself. As a result, here again we must consider that the grafting between the anionic functions of organic anion and the hydroxyled layers through the moderate modification of coordination modes has occurred at medium-temperature for the hydrothermal treatment, and results in the condensation of layers.

The presence of grafting process is also evidenced on the TGA–DTG plots for the intercalated LDH and the hydrothermally-treated sample at 120 °C. Fig. 6 shows the result of the TGA–DTG analysis of the samples as a function of temperature. Note that the TGA traces for two samples indicate two and three general regions of mass loss, respectively, corresponding two and three obvious peaks in the DTG curves. Indeed, before 300 °C, the weight loss appears from room temperature to 250 °C as a continuous step for the intercalated sample corresponding to desorption of physisorbed and interlayer water molecules, but two separated events for the treated sample appear in the range of room temperature to 150 and 160–290 °C, individually. This may be because of the fact that interlayer anions in the treated sample have been densely held and packed in the interlayer domain with the loss of the hydrogen-bonding domain on both side of the layers, and thus interlayer water molecules are limited in a smaller region, as implies that the grafting process should be involved in the treated sample. Meanwhile, only a DTG peak in the range of 350–600 °C corresponding to the dehydroxylation of the lattices and decomposition of the interlayer anions is observed for the untreated sample, however, the corresponding processes for the treated one result in splitting doublet DTG peaks at higher temperature. It implies that the interlayer anions interact more strongly with the backbone in the treated sample. The split of DTG peak can be attributed to the symmetry degradation of the interlayer anions, which probably results from two types of coordination modes of the organic functions.

In order to investigate the local chemical environment of anionic $-PO_3^{2-}$ functions of Gly anions in the brucite-like layers, the ^{31}P MAS NMR spectra of MgAl–Gly–LDH and the treated hydrothermally-treated sample at 120 °C were recorded in Fig. 7. The ^{31}P MAS NMR spectrum of MgAl–Gly–LDH shows a sharp resonance at around 22.75 ppm. However, as shown in Fig. 7, the chemical shift of the ^{31}P nucleus for sample displaces to lower field after hydrothermal treatment. The result is consistent with the assumption that upon hydrothermal treatment the electronic density of the P–O bond decreases, as the anionic $-PO_3^{2-}$ functions of Gly anions are linked onto the lattices of LDH.

To further confirm the presence of the grafting process, the anion exchange with carbonate anions for the sample treated hydrothermally at 120 °C was carried out. The powder XRD patterns for MgAl–CO_3–LDH and the exchanged sample are present in Fig. 8. It is seen that after anion exchange with carbonate for the treated sample, the positions of the characteristic diffractions are almost the same as those before anion exchange (see Fig. 4c) with no presence of the characteristic diffractions for MgAl–CO_3–LDH. The result suggests the Gly/carbonate exchange has been hindered due

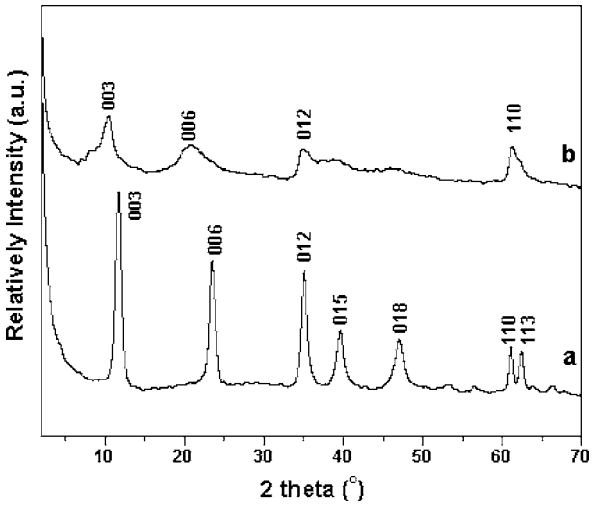

Fig. 8. XRD patterns for: (a) MgAl–CO_3–LDH and (b) MgAl–Gly–LDH treated hydrothermally at 120 °C after ion exchange with carbonate.

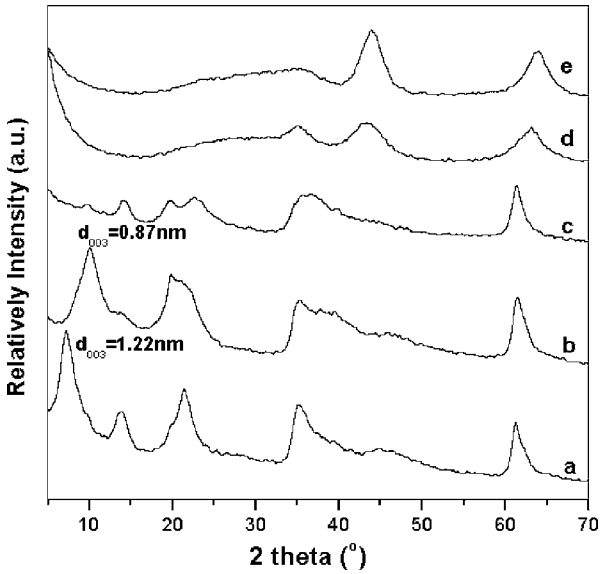

Fig. 9. XRD patterns for MgAl–Gly–LDH at different calcinations temperature: (a) room temperature, (b) 120 °C, (c) 350 °C, (d) 500 °C and (e) 700 °C.

to the grafted Gly anions, although carbonate has a large affinity for LDHs containing Mg and Al.

To our knowledge, two types of grafting reactions on layered structures have been described in the literature, both a topotactic ionic exchange of pending groups, often promoted by acid hydrolysis [31] and a condensation reaction of adsorbed or intercalated molecules with oxychloride or hydroxy layers [32]. Few studies have been reported about grafting of organic molecules on the hydroxylated layers of LDHs with a strong ion–covalent M–O-organic bonding. Moriaka et al. reported a reaction with acylchloride RCOCl [33]. All the other papers deal with the reactivity of phophonates [34–38]. For example, Wang et al. [34] and Clearfield et al. [38] obtained the grafting after a thermal treatment of a phosphonate intercalated MgAl (d_{003} = 1.33 nm), and the temperature of condensation seems to be dependent on the thermal stability of the LDH layers. In our case, at low temperature, the organic species enter the interlayer space only to displace the interlamellar anions and then are held loosely between the LDH layers. As soon as the compound is treated thermally, the lower *d*-spacing product appears as dehydration removed the OH^- groups from the layer, leading to the grafted products in which the anionic $–PO_3^{2-}$ and $–CO_2^-$ functions of Gly anions connect directly to the metal cations in the LDH sheets, no longer through the OH^- groups. As a result, the proposed hypothesis of the grafting reaction is as follows:

$$[\text{LDH}]–\text{OH} + \text{R}–\text{COO}^- \xrightarrow{120–150\,^\circ\text{C}} [\text{LDH}]–\text{O}–\text{COR} + \text{HO}^-$$

$$[\text{LDH}]–\text{OH} + \text{R}–\text{PO}_3^{2-} \xrightarrow{120–150\,^\circ\text{C}} [\text{LDH}]–\text{O}–\text{PO}_2\text{R}^- + \text{HO}^-$$

$$[\text{LDH}]–\text{OH} + \text{HO}^- \xrightarrow{120–150\,^\circ\text{C}} [\text{LDH}]–\text{O}^- + \text{H}_2\text{O}$$

Fig. 2b gives a schematic representation of this hypothesis, where the association between both grafted organic anions and inorganic layers of the host structure can form a single hybrid phase, and a different orientation of grafted Gly anions is proposed as a tilted arrangement to the lattice in interlayer domain of LDH.

3.3. Thermal decomposition

The XRD patterns for MgAl–Gly–LDH and resulting calcined samples at 120, 350, 500 and 700 °C, respectively, are distinguished and presented in Fig. 9. The XRD patterns for the calcined sample at 120 °C keep the typical characteristic diffractions of a hydrotalcite-like LDH material. However, its (0 0 *l*) diffraction lines are obviously broadened, suggesting a disorder in the layers stacking and a loss of the crystalline order. The result could be accounted by loss of the loosely held interlayer water molecules and grafting reaction of interlayer Gly anions, resulting in a shift of d_{003} from 1.22 to 0.87 nm with the gallery height of 0.39 nm close to that of the samples treated hydrothermally at 120 and 150 °C discussed above. Due to the loss of an amount of OH groups on the lattices of LDH, calcination of LDHs at 350 °C affords a poorly crystalline layered phase. On heating at 500 °C or above, all (0 0 *l*) diffraction lines of XRD pattern vanish due to the complete decomposition of the interlayer anions, and thus the XRD patterns in Fig. 9d and e present only a series of broad diffraction lines close to those of periclase MgO, which can be described as MgO-like phase [39]. It is proposed that the broadening of the XRD diffractions of MgO-like phase is due to poor crystallinity or small particle size, or to both [40].

It is also interesting to investigate how the changes in the number and type of functional groups with temperature manifest themselves in changes in the crystal structure of the

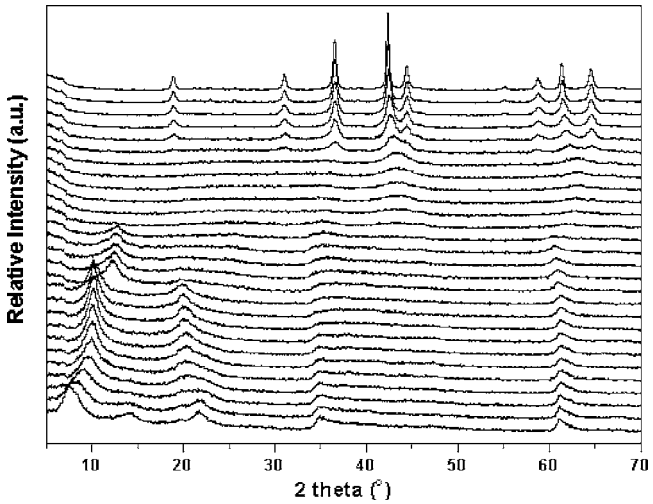

Fig. 10. In situ HT-XRD patterns for MgAl–Gly–LDH between 25 and 1200 °C temperature from top to bottom are (°C): 1200 (top); 1150, 1100, 1050, 1000, 900, 800, 700, 650, 600, 550, 500, 450, 400, 360, 320, 280, 240, 200, 180, 160, 140, 120, 100, 80, 60, 40 and 25 (bottom).

MgAl–Gly–LDH. In order to study this, in situ HT-XRD has been utilized. A general view in Fig. 10 shows the whole in situ HT-XRD patterns for the MgAl–Gly–LDH between 25 and 1200 °C. Apparently, there are five temperature regions which are classified by the common HT–XRD pattern in each region: (1) 25 °C ≤ T ≤ 100 °C; (2) 120 °C ≤ T ≤ 240 °C; (3) 280 °C ≤ T ≤ 450 °C; (4) 500 °C ≤ T ≤ 800 °C; and (5) 900 °C ≤ T ≤ 1200 °C.

The HT-XRD patterns in the first temperature region, whose diffraction lines are the well-known hydrotalcite-like layered structure of LDH (phase I), agree with the XRD data discussed above. Note that with the elevated temperatures the (0 0 3) diffraction line at 7.46° starts shifting towards around 9.64°. Meanwhile, the initial (0 0 6) diffraction line at 14.14° disappears gradually, and the (0 0 9) diffraction line at 21.67° shifts gradually towards lower angle up to 20.28°, which is approximately two times of 2θ angel of 9.64° for the (0 0 3) diffraction line, as suggests that other layered phase begins to form gradually. The decrease of the basal spacing can be attributed to the shrinkage of layers due to the removal of physisorbed and interlayer water molecules, and grafting process. This structure of phase I disappears completely at 120 °C, and another new phase (phase II) with sharp and intense (0 0 3) diffraction line around 10.07° exists in the second temperature region 120–240 °C. At these temperatures, the X-ray diffraction patterns are not appreciably modified, indicating that the layered structure with a smaller basal spacing is stable. Moreover, the XRD patterns for phase II with only two 0 0 l-type diffraction lines is common to those for the thermally treated samples at 120 °C. The smaller value of the basal spacing suggests strongly that the interlayer species are different from each other in the two solid phases (phase I and phase II), and thus a grafted hybrid compound is formed in phase II. However, the grafting does not affect markedly the layered structure because it concerns only the substitution of a low fraction of the amount of total OH groups. In the third temperature region of 280–450 °C, the diffraction line around 10.07° disappears, and simultaneously the diffraction line around 12.31° appears and shifts gradually towards 12.93°. This means that in this region phase II transforms to another transition phase, as may be attributed to the removal of OH groups on the lattice. With increasing temperature, the transition phase falls apart and collapses completely above 450 °C. In the forth temperature region, a phase ascribed to an MgO-like phase was formed, as mentioned above, and the intensity of the diffraction lines increase with temperature up to 800 °C. Above 900 °C, the diffractogram reveals an $MgAl_2O_4$ spinel-type phase with increasing crystallinity at temperatures up to 1200 °C.

4. Conclusion

We have successfully synthesized layered double hydroxide intercalated with trivalent and divalent glyphosate anions through anion exchange and coprecipitation methods. When the intercalated sample with a basal spacing of 1.22 nm is submitted to thermal treatments (hydrothermal treatments and calcinations) at 120 °C or above, strong contraction of the basal spacing was observed for the organic–inorganic hybrid phase with interlayer domain filled with large organic anions densely packed. The decrease in the basal spacing arises obviously from grafting reaction of anionic functions (carboxylate and phosphonate) of interlayer glyphosate anions with hydroxyl groups on the layers of the host structure. Under the thermal decomposition, the organic–inorganic hydride phase is metastable. With elevated temperature, a series of processes including desorption of physisorbed and interlayer water, grafting of interlayer anions onto the lattice, dehydroxylation of the lattice and decomposition of interlayer Gly anions, will lead to a variety of crystallographic transitions.

Acknowledgements

We gratefully acknowledge the financial support from the National Natural Science Foundation of China (No. 20306003) and the Beijing Nova Program (No. 2003B10).

References

[1] Z. Gerstl, Behavior of organic agrochemicals in irrigated solids, in: M.L. Richardson (Eds.), Chemistry, Agriculture and the Environment, The Royal Society of Chemistry, Cambridge, UK, 1991, pp. 332.
[2] C. Guyot, Strategies to minimize the pollution of water by pesticides, in: H. Borner (Eds.), Pesticides in Ground Water and Surface Water, Chemistry of Plant Protection, vol. 9, Springer–Verlag, Berlin, 1994.
[3] M.J.S. Martín, M.V. Villa, M. Sanchez-Camazano, Clays Clay Miner. 6 (1999) 777.

[4] Z. Gerstal, A. Nasser, U. Mingelgrin, J. Agric. Food Chem. 46 (1998) 3803.
[5] A. de Roy, C. Forano, K.E.I. Malki, J.P. Besse, Expanded clays and other microporous solids, in: M.L. Occelli, H. Robson (Eds.), Synthesis of Microporous Materials, Van Nostrand Reinhold, New York, 1992, Chapter 7.
[6] F. Cavani, F. Trifiróand, A. Vaccari, Catal. Today 11 (1991) 173.
[7] J.L. Atwood, J.E. Davies, D.D. MacNicol, F. Vogtle (Eds.), in: Comprehensive Supramolecular Chemistry, Pergamon, Elmsford, New York, 1997, Chapter 7.
[8] F. Malherbe, J.P. Besse, J. Solid State Chem. 155 (2000) 332.
[9] E.W. Serwicka, P. Nowak, K. Bahranowski, W. Jones, F. Kooli, J. Mater. Chem. 7 (1997) 1937.
[10] N.T. Whilton, P.J. Vickers, S. Mann, J. Mater. Chem. 7 (1997) 1623.
[11] S.P. Newman, W. Jones, New J. Chem. 22 (1998) 105.
[12] F. Leroux, J.P. Besse, Chem. Mater. 13 (2001) 3507.
[13] H.T. Zhao, G.F. Vance, Clays Clay Miner. 46 (1998) 712.
[14] W.P. Ding, G. Gu, W. Zhong, W.C. Zang, Y.W. Du, Chem. Phys. Lett. 262 (1996) 259.
[15] B. Sels, D. De Vos, M. Buntinx, F. Pierard, A. Kirsch-De Mesmaeker, P. Jacobs, Nature 400 (1999) 855.
[16] M. Ogawa, K. Kuroda, Chem. Rev. 95 (1995) 399.
[17] S.P. Newman, W. Jones, Supramolecular Organization and Materials Design, in: C.N.R. Rao, W. Jones (Eds.), Cambridge University Press, Cambridge, UK, 2001, pp. 295.
[18] A.M. Fogg, V.M. Green, H.G. Harvey, D. O'Hare, Adv. Mater. 11 (1999) 1466.
[19] F. Millange, R.I. Walton, L.X. Lei, D. O'Hare, Chem. Mater. 12 (2000) 1990.
[20] El.M. Moujahid, M. Dubois, J.P. Besse, F. Leroux, Chem. Mater. 14 (2002) 3799.
[21] H. Tagaya, S. Sato, T. Kuwahara, J. Kadokawa, K. Masa, K. Chiba, J. Mater. Chem. 4 (2002) 1907.
[22] C. Busetto, G. Del Piero, G. Mamara, F. Trifiró, A. Vaccari, J. Catal. 85 (1984) 260.
[23] A. Sumio, T. Satoshi, O. Wataru, U. Yoshio, N. Eiichi, J. Solid State Chem. 162 (2001) 52.
[24] P. Kaliannan, M. Mohamed Naseer Ali, T. Seethalakshmi, P. Venuvanalingam, J. Mol. Struct. (Theochem.) 618 (2002) 117.
[25] K. Nakamoto, Infrared and Raman Spectra of Inorganic and Coordination Compounds, Wiley, New York, 1986.
[26] J.T. Kloprogge, R.L. Frost, J. Solid State Chem. 146 (1999) 506.
[27] D.L. Bish, G.W. Brindley, Am. Mineral. 62 (1977) 458.
[28] M. Khaldi, M. Badreddine, A. Legrouri, M. Chaouch, A. Barroug, A.De. Roy, J.P. Besse, Mater. Res. Bull. 33 (1998) 1835.
[29] M.K. Titulaer, J.B.H. Jansen, J.W. Geus, Clays Clay Miner. 42 (1994) 249.
[30] S. Aisawa, S. Takahashi, W. Ogasawara, Y. Umetsu, E. Narita, J. Solid State Chem. 162 (2001) 52.
[31] G. Alberti, M. Bartocci, M. Santarelli, R. Vivani, Inorg. Chem. 36 (1997) 2844.
[32] B. Bujoli, P. Janvier, J. Villeras, P. Palvadeau, J. Rouxel, Lamellar ferric oxychloride properties from intercalation to topochemical reactions, in: A.P. Legrand, S. Flandrois (Eds.), Chemical Physics of Intercalation, NATO ASI Ser. B, Phys. 172, 1987, pp. 411.
[33] H. Moriaka, H. Tagaya, M. Karasu, J. Kadokawa, K. Chiba, J. Solid State Chem. 117 (1995) 337.
[34] J.D. Wang, G. Serrette, Y. Tian, A. Clearfield, Appl. Clay Sci. 10 (1995) 103.
[35] F.M. Vichi, O.L. Alves, J. Mater. Chem. 7 (1997) 1631.
[36] S. Carlino, M.J. Hudson, S. Waqif Husain, J.A. Knowles, Solid State Ion. 84 (1996) 117.
[37] U. Constantino, M. Casciola, L. Massilini, M. Nocchetti, R. Vivani, Solid State Ion. 97 (1997) 203.
[38] H. Nijs, A. Clearfield, E.F. Vansant, Microporous Mesoporous Mater. 23 (1998) 97.
[39] J.C.A.A. Roelofs, J.A. Van Bokhoven, A. Jos van Dillen, J.W. Geus, K.P. de Jong, Chem. Eur. J. 8 (2002) 5571.
[40] K.J.D. Mackenzie, R.H. Meinhold, B.L. Sherriff, Z. Xu, J. Mater. Chem. 3 (1993) 1263.